# MODELLING OF CATALYST PELLET DEACTIVATION

Alena Brunovská[a], Ján BURIÁNEK[a], Ján ILAVSKÝ[a] and Ján VALTÝNI[b]

[a] *Department of Organic Technology,*
*Slovak Institute of Technology, 812 37 Bratislava and*
[b] *Department of Inorganic Technology,*
*Slovak Institute of Technology, 812 39 Bratislava*

The diffusion and the shell progressive models of deactivation caused by irreversible chemisorption of a catalytic poison are presented for a single catalyst pellet. The method for solution of the model equations is proposed. The numerical results are compared with experimental data obtained by measuring concentration and temperature changes due to thiophene poisoning in benzene hydrogenation over a nickel–alumina catalyst.

This paper deals with the problem of the mechanism of catalyst pellets deactivation. The interaction of the chemical and physical processes taking place in a porous catalyst may give rise to unexpected phenomena, for instance the temperature in the bed in the course of the deactivation process may exceed the adiabatic temperature[1]. Due to decrease of the catalyst activity the temperature and the concentration profiles move downstream through the reactor. The movement mode is not only a function of the reactor type and working conditions, but also of the deactivation mechanism.

A heterogeneous model of a catalytic reactor has to include the balance of the catalyst pellet. If the deactivation process takes place in the reactor, it is necessary to know this process on one pellet. Since numerical solution of heterogeneous models is involved, we would like to describe the process in a catalyst pellet as simple as possible.

Partial investigations of deactivation problems have been reported in[2-5], where temperature in the catalyst pellet during the deactivation process has been studied. In[2-4], the temperature profiles in the pellet at the initial period of the reaction on the fresh and partialy deactivated catalyst have been described. As the mass balance of the poison the diffusion-reaction equation with the deactivation rate relation of the first order has been employed. In[6], the isothermal diffusion model with various poisoning mechanisms has been studied. In[7,8], the formulation of the isothermal diffusion model for the case of irreversible chemisorption of the catalytic poison (so called "side-by-side" mechanism) and its comparison with the shell progressive or pore-mouth model can be found. The deactivation kinetics and the

pellet effectiveness factor for the slab geometry in the limiting case of uniform and pore-mouth deactivation have been developed in[9].

In this paper our studies of deactivation caused by irreversible chemisorption of catalyst poison which comes from some impurity in the feed are presented. The aim is to develop several models of catalytic reaction and deactivation of one pellet together with the balances of the reactor in dimensionless form, to work out effective numerical algorithms for their solution and to compare the experimental and numerical results.

### THEORETICAL

The models of catalyst pellet deactivation developed below are valid under following assumption: *1*) All catalyst pellet properties are isotropic and except of catalyst activity independent of the deactivation level. *2*) The heat of the reaction, heat capacity, diffusion coefficients, and thermal conductivity are temperature independent. *3*) The catalyst poison concentration is considerably lower than the concentration of the key component, so the heat released by the chemisorption of the poison compared to the heat released by the reaction is negligible. *4*) The reaction rate equation is separable[10]. *5*) Catalyst activity depends linearly on the adsorbed amount of the catalyst poison. *6*) The rate of poison adsorption is independent of the rate of the catalytic reaction.

Two basic model ideas of the catalyst pellet deactivation are considered, the first being the "diffusion", the second the "shell progessive" models. In the diffusion models the catalyst poison balance is described by the diffusion equation, which leads to continuous activity and poison distribution through the pellet. The shell progressive model corresponds to the shrinking core model for noncatalytic gas–solid reactions. In this model the pellet consists of a unpoisoned core with unit activity surrounded by completely poisoned shell with zero activity. The border of the activity core and nonactive shell is moving towards the center of the pellet with time.

*Diffusion Model (Model* 1)

First we will investigate the diffusion model[2-4]. The model consists of the following equations:
mass balance of the key component

$$\varepsilon \frac{\partial c_B}{\partial t} = D_B \nabla^2 c_B + v_B \dot{\zeta}_z \qquad (1)$$

mass balance of the poison

$$\varepsilon \frac{\partial c_J}{\partial t} + \frac{\partial a_J}{\partial t} = D_J \nabla^2 c_J \qquad (2)$$

enthalpy balance

$$\varrho C_{\mathrm{p}} \frac{\partial T}{\partial t} = \lambda \nabla^2 T + (-\Delta H) \dot{\xi}_{\mathrm{Z}} \tag{3}$$

rate equation of the catalytic reaction

$$\dot{\xi}_{\mathrm{Z}} = \phi(a_{\mathrm{J}}) f(c_{\mathrm{A}}, c_{\mathrm{B}}, \ldots, T) \tag{4}$$

deactivation rate

$$\frac{\mathrm{d}a_{\mathrm{J}}}{\mathrm{d}t} = g(a_{\mathrm{J}}, c_{\mathrm{J}}, T) \tag{5}$$

boundary conditions

$$r = 0 ; \quad \nabla c_{\mathrm{i}} = \nabla T = 0 \tag{6}$$

$$r = R ; \quad c_{\mathrm{i}} = c_{\mathrm{i}}^{*} , \quad \lambda \left(\frac{\partial T}{\partial r}\right) = \alpha(T_{\mathrm{g}} - T) . \tag{7}$$

The initial conditions are given by the solution of Eqs $(1)-(7)$ for the steady state conditions and fresh catalyst.

If the catalyst activity depends linearly on the adsorbed amount of the poison, it is given by

$$\phi = \frac{a_{\mathrm{J}}^0 - a_{\mathrm{J}}}{a_{\mathrm{J}}^0} . \tag{8}$$

Assuming quasi-steady state (the deactivation rate is much lower than the rate of the catalytic reaction) and introducing dimensionless variables and parameters

$$Y_{\mathrm{B}} = c_{\mathrm{B}}/c_{\mathrm{B0}} , \quad Y_{\mathrm{J}} = c_{\mathrm{J}}/c_{\mathrm{J0}} , \quad \vartheta = (T - T_{\mathrm{g}})/\Delta T_{\mathrm{m}} \tag{9}$$

$$\tau = t/t^0 , \quad \varphi = r/R , \quad \dot{\Xi} = \dot{\xi}_{\mathrm{Z}}/\dot{\xi}_{\mathrm{Z}}^0$$

$$Th_{\mathrm{B}} = R \sqrt{\left[\frac{\dot{\xi}_{\mathrm{Z}}^0(-\nu_{\mathrm{B}})}{D_{\mathrm{B}}c_{\mathrm{B0}}}\right]} , \quad Th_{\mathrm{J}} = R \sqrt{\left(\frac{a_{\mathrm{J}}^0}{D_{\mathrm{J}}c_{\mathrm{J0}}t^0}\right)} , \quad Bi = \alpha R/\lambda$$

the system of the model Eqs $(1)-(7)$ becomes

$$Th_{\mathrm{B}}^2 \dot{\Xi} = \nabla^2 Y_{\mathrm{B}} \tag{10}$$

$$-Th_{\mathrm{J}}^2 \dot{\phi} = \nabla^2 Y_{\mathrm{J}} \tag{11}$$

$$-Th_{\mathrm{B}}^2 \dot{\Xi} = \nabla^2 \vartheta \tag{12}$$

(material balances and enthalpy balance)

$$\dot{\Xi} = \phi f(Y_A, Y_B, ..., \vartheta) \tag{13}$$

(reaction rate equation)

$$\dot{\phi} = \frac{d\phi}{d\tau} = g(\phi, Y_J, \vartheta) \tag{14}$$

(deactivation rate)

$$\varphi = 0 ; \quad \nabla Y_i = \nabla \vartheta = 0 \tag{15}$$

$$\varphi = 1 ; \quad Y_i = Y_i^* , \quad (\partial \vartheta / \partial \varphi) = -Bi\vartheta \tag{16}$$

(boundary conditions).

The dimensionless temperature $\vartheta$ is normalized by the maximum temperature rise in the pellet $\Delta T_m$

$$\Delta T_m = \frac{(-\Delta H) D_B c_{B0}}{\lambda(-\nu_B)} \tag{17}$$

and the time $\tau$ by the characteristic deactication time $t^0$ the concrete expression of which depends on the rate equation for deactivation.

*Diffusion Model with Uniform Temperature in the Pellet (Model 2)*

The material balances are given by Eqs (10) and (11). After introducing the assumption of uniform temperature in the pellet, considering only external heat transfer resistance, the enthalpy balance (quasi-steady state; cylindrical shape of the pellet) becomes

$$\frac{1}{(-\nu_B)} D_B \left(\frac{\partial c_B}{\partial r}\right)_{r=R} (-\Delta H) = \alpha(T - T_g) \tag{18}$$

and in the dimensionless form

$$\vartheta = \frac{2}{Th_B^2} \left(\frac{\partial Y_B}{\partial \varphi}\right)_{\varphi=1} . \tag{19}$$

The dimensionless temperature $\vartheta$ is again normalized by the maximum temperature rise (for $\lambda \to \infty$) (ref.[11])

$$\Delta T_m = \frac{\dot{\xi}_Z^0 (-\Delta H) R}{2\alpha} . \tag{20}$$

The models *1* and *2* have been developed using the deactivation rate

$$\frac{\mathrm{d}\phi}{\mathrm{d}t} = -k_J\phi c_J \tag{21}$$

which is in the dimensionless form

$$\dot{\phi} = -\phi Y_J. \tag{22}$$

The characteristic deactivation time $t^0$ is

$$t^0 = 1/(k_J c_{J0}). \tag{23}$$

*Shell Progressive Model (Model 3 and 4)*

In the models below we will consider shell progressive poisoning of catalyst pellet under quasi-steady state conditions[7,8]. The suggested model includes diffusion through the shell and chemisorption on the border of the shell and core, the ratio of the chemisorption being

$$\omega = \frac{a_J^0 R}{c_{J0} k_S t^0}. \tag{24}$$

If we denote by $\varphi^j$ the radius of the active core, for the infinite cylinder pellet we can write

$$\frac{\mathrm{d}\varphi^j}{\mathrm{d}\tau} = -\frac{Y_J^*}{\omega - (1 - \omega)\,\varphi^j \ln \varphi^j}. \tag{25}$$

In this case the characteristic time for deactivation is

$$t^0 = \frac{a_J^0 R}{c_{J0}}\left(\frac{1}{k_S} + \frac{R}{D_J}\right). \tag{26}$$

The limiting cases are:

$$\omega = 1 \; ; \quad \dot{\varphi}^j = -Y_J^* \quad \text{(diffusion-free surface reaction)}$$

$$\omega = 0 \; ; \quad \dot{\varphi}^j = -Y_J^*/(\varphi^j \ln(1/\varphi^j)) \quad \text{(diffusion limited reaction)}.$$

The mean pellet activity is $\bar{\phi} = \varphi^{j2}$. The concentration profile of the poison in the shell $Y_J$ we obtain from the solution of the equation

$$\nabla^2 Y_J = 0 \tag{27}$$

which for the considered geometry of the pellet is

$$Y_J = Y_J^* - (Y_J^* - Y_J^j) \ln \varphi / \ln \varphi^j , \qquad (28)$$

where

$$Y_J^j = \frac{Y_J^*}{1 + ((1 - \omega)/\omega) \varphi^j \ln (1/\varphi^j)} \qquad (29)$$

is the core boundary concentration of poison. The concentration of the key component in the core and in the shell are given by Eq $(10)$ and

$$Y_B = Y_B^* - (Y_B^* - Y_B^j) \ln \varphi / \ln \varphi^j . \qquad (30)$$

respectively. The relation between core boundary concentration and concentration on the pellet surface is

$$Y_B^j = Y_B^* + \frac{Th_B^2}{2} \dot{\bar{\Xi}} \ln \varphi^j . \qquad (31)$$

The enthalpy balance can be considered either in the form of Eq. $(12)$ (Model $3$) or, under the assumption of uniform temperature in the pellet (Model $4$) in the form

$$\dot{\xi}_Z(-\Delta H) R = 2\alpha(T - T_g) . \qquad (32)$$

In the dimensionless form Eq. $(32)$ becomes

$$\vartheta = \bar{\Xi} . \qquad (33)$$

*Shell progressive model with constant effectiveness factor in the core* (*Model* 5)

The simplest model of catalyst pellet deactivation assumes shell progressive poisoning and constant effectiveness factor of the active core. Then the mean rate of catalytic reaction is

$$\bar{\Xi} = \eta \dot{\Xi}(Y_B^*, \vartheta) \varphi^{j2} \qquad (34)$$

and the enthalpy balance is in the form $(33)$.

*Reactor Balances*

The surface concentration and bulk flow temperature are given by the experiment. If the pellet is placed in a continuous stirred tank reactor with constant temperature

of the bulk flow, the system of the model equations has to be extended by the material balances of the reactor

$$\dot{V}c_{B0} + v_B\bar{\xi}_ZW/\varrho = \dot{V}c_B^* + V\,dc_B^*/dt\,,\tag{35}$$

$$\dot{V}c_{J0} - \bar{a}_JW/\varrho = \dot{V}c_J^* + V\,dc_J^*/dt\,.\tag{36}$$

Assuming quasi-steady state conditions and introducing dimensionless variables Eqs (35) and (36) become

$$1 - Z_R\bar{\Xi} = Y_B^*\,,\tag{37}$$

$$1 + G\bar{\phi} = Y_J^*\,,\tag{38}$$

where

$$Z_R = \frac{\xi_Z^0W(-v_B)}{\dot{V}c_{B0}\varrho} \quad\text{and}\quad G = \frac{a_J^0W}{\dot{V}c_{J0}t^0\varrho}\,.\tag{39}$$

For the diffusion models Eqs (37) and (38) yield the boundary conditions

$$\left(\frac{\partial Y_B}{\partial\varphi}\right)_{\varphi=1} = \frac{1 - Y_B^*}{Z_R}\frac{Th_B^2}{2}\,,\tag{40}$$

$$\left(\frac{\partial Y_J}{\partial\varphi}\right)_{\varphi=1} = \frac{1 - Y_J^*}{G}\frac{Th_J^2}{2}\,,\tag{41}$$

for the shell progressive models they yield

$$\left(\frac{\partial Y_B}{\partial\varphi}\right)_{\varphi=\varphi^j} = \frac{1 - Y_B^*}{Z_R}\frac{Th_B^2}{2\varphi^j}\,.\tag{42}$$

The enthalpy balance in models 2, 4, and 5 is

$$\vartheta = \frac{1 - Y_B^*}{Z_R}\,.\tag{43}$$

*Rate Equation*

The rate equation of the catalytic reaction in dimensionless form[12] has been used

$$\dot{\Xi} = \phi\frac{(1 + \varkappa_B)\,Y_BY_H\exp\left[(\alpha_i + \alpha_k)\,\beta\vartheta/(1 + \beta\vartheta)\right]}{1 + \varkappa_BY_B\exp\left[\alpha_k\beta\vartheta/(1 + \beta\vartheta)\right]}\,,\tag{44}$$

where

$$\varkappa_B = K_\infty c_{B0} \exp\left[-Q/(RT_0)\right]$$
$$\alpha_i = E/(RT_0)$$
$$\alpha_k = Q/(RT_0)$$
$$\beta = \Delta T_m / T_0 .$$

(45)

## EXPERIMENTAL

The catalyst pellet has been placed in the continuous stirred tank reactor in such a way that the reacting gas has been in contact with the lateral surface of the cylinder only. The gaseous phase of volume 100 ml has been intensively mixed in order to enable us to assume uniform concentration through the reactor and to neglect external diffusion. The temperature in the reactor has been regulated, the temperature inside the pellet has been measured by four iron-copper thermocouples. The concentration in the outflowing stream has been measured during the experiment by a gas chromatograph.

Benzene hydrogenation on a Ni-catalyst (Ni-alumina, 58% Ni) was applied as the model reaction system and thiophene as the catalyst poison. The catalyst pellet has been preconditioned at 180°C for a period 12 h in the flow of hydrogen (50 ml min$^{-1}$). After activating the catalyst and decreasing the temperature to the required value, benzene and hydrogen have been fed to the reactor. After stabilizing the conditions, the inlet has been switched to a thiophene containing feed. The experimental conditions are in Table I.

## NUMERICAL SOLUTION

*Models* 1 *and* 2. The system of the model equations has been solved iteratively. The space derivatives $\nabla^2 Y_i$ have been replaced by virtual profile finite-differences and nonlinear terms $(\dot\Xi$ and $\dot\phi)$ have been computed from the two previous iterations. The activity profile at time $\tau + \Delta\tau$ has been computed from Eq. (22), by the explicit finite difference scheme

$$\phi(\varphi, \tau + \Delta\tau) = \phi(\varphi, \tau) - \Delta\tau \dot\phi(\varphi, \tau) .$$

(46)

TABLE I

Experimental conditions

| Run | 1 | 2 | 3 |
|---|---|---|---|
| Catalyst radius (mm) | 7·55 | 7·55 | 7·55 |
| Catalyst mass (g) | 3·211 | 3·011 | 2·903 |
| Bulk flow temperature (°C) | 98·0 | 121·0 | 93·4 |
| Volumetric flow rate ($10^6$ m$^3$ s$^{-1}$) | 1·86 | 1·86 | 1·87 |
| Inlet benzene concentration (mol m$^{-3}$) | 2·374 | 2·366 | 2·383 |
| Inlet thiophene concentration ($10^2$ mol m$^{-3}$) | 7·78 | 7·75 | 4·38 |

The temperature inside the pellet in model *1* has been computed as follows: The Eqs $(10)$ and $(12)$ lead to the relation

$$\nabla^2 Y_B + \nabla^2 \vartheta = \nabla^2 z = 0 , \tag{47}$$

where we denote $z = Y_B + \vartheta$. From the symmetry conditions $(15)$ it follows that at any time instant the variable $z$ is constant through the pellet and equal to its surface value.

From the boundary conditions $(16)$ one obtains

$$z = \frac{1 - Y_B^*}{2 Z_R Bi} Th_B^2 + Y_B^* . \tag{48}$$

The temperature in the model *2* has been computed from Eq. $(43)$.

TABLE II
Dimensionless model parameters

| | Run | 1 | 2 | 3 |
|---|---|---|---|---|
| $\alpha_i$ | | 11·459 | 10·791 | 11·603 |
| $\alpha_k$ | | −7·850 | −7·392 | −7·949 |
| $\varkappa_B$ | | 42·922 | 27·150 | 48·202 |
| $Z_R$ | | 5·562 | 9·998 | 4·251 |
| $Th_B^2$ | Models *1, 3* | 580 | 1 034 | 650 |
| | Models *2, 4* | 590 | 1 060 | 666 |
| | Model *4* — shell | 105 | 260 | 50 |
| | Model *4* — core | 590 | 1 060 | 666 |
| $Th_J^2$ | Models *1, 2* | 182 | 167 | 243 |
| $\omega$ | Models *3, 4, 5* | 0·07 | 0·09 | 0·06 |
| $Bi$ | Models *1, 3* | 90 | 90 | 90 |
| $G$ | Models *1, 2* | 14 | 12 | 12 |
| | Models *3, 4, 5* | 0·0676 | 0·0793 | 0·0441 |
| $\beta$ | Models *1, 3* | 0·0040 | 0·0118 | 0·0069 |
| | Models *2, 4, 5* | 0·0414 | 0·1694 | 0·0784 |
| $\eta$ | Model *5* | 0·079 | 0·051 | 0·078 |

*Models* 3 *and* 4. The solution of the Eqs $(25)$, $(38)$ and the relation for the mean deactivation rate $\bar{\phi} = 2\varphi^j\dot{\phi}^j$ can be expressed by the formulas

$$\tau = \omega(1 - \varphi^j) + \left(G + \frac{1 - \omega}{4}\right)(1 - \varphi^{j2}) + (1 - \omega)\frac{\varphi^{j2}}{2}\ln\varphi^j, \qquad (49)$$
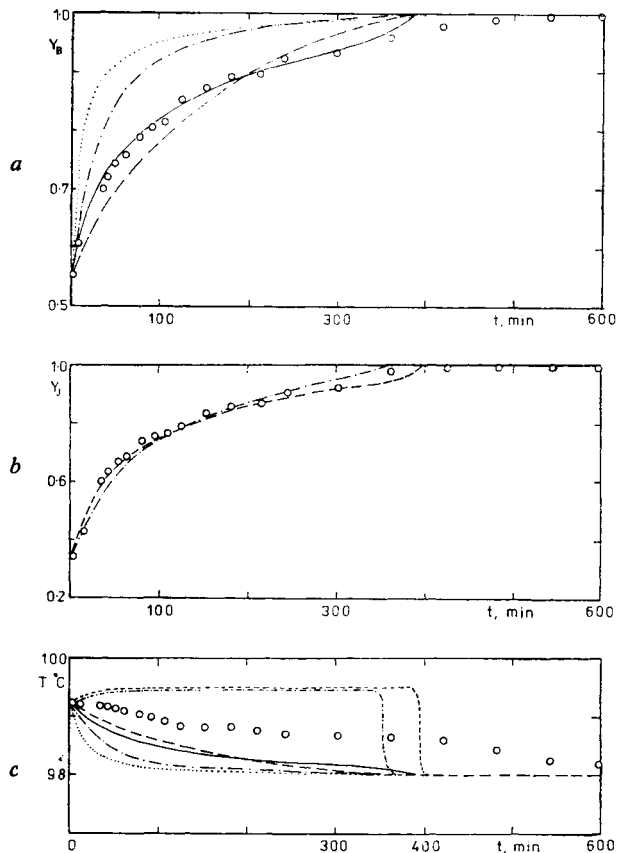


FIG. 1

Experimental run 1. *a*) Benzene concentration *vs* time. $-\cdot-\cdot-$ Models *1*, *2*, $\cdots\cdots$ Models *3*, *4*, $-----$ Model *5*, ——— Model *4* — differrent Thiele modulus for benzene of core and shell. *b*) Thiophene concentration *vs* time. $-\cdot-\cdot-\cdot$ Models *1*, *2*, $-----$ Models *3*, *4*, *5*. *c*) Temperature in the pellet center *vs* time. $-\cdot-\cdot-\cdot$ Model *1*, $—\cdot—\cdot—$ Model *2*, $-----$ Model *3*, $\cdots\cdots$ Model *4*, $----$ Model *5*, ——— Model *4* — different Thiele modulus for benzene of core and shell

$$Y_J^* = \frac{\omega - (1 - \omega)\,\varphi^j \ln \varphi^j}{\omega - (1 - \omega)\,\varphi^j \ln \varphi^j + 2G\varphi^j}.$$ (50)

For a given active core radius $\varphi^j$, $\tau$ and $Y_J^*$ have been computed from Eqs (49) and (50). The profile of $Y_B$ and $\vartheta$ one obtains by solving numerically Eqs (10), (30), (31), (37), (42), (44), (48) for model 3 and Eqs (10), (30), (31), (37), (42)—(44) for model 4 by the following iteration scheme: Choose the surface concentration $Y_B^*$ and compute the values of $z$ and $\vartheta^*$. From the boundary condition (42) and Eq. (10) compute the profile inside the active core. If the choice of $Y_B^*$ was correct, the material balance of the reactor (37) and boundary condition (15) must be satisfied.
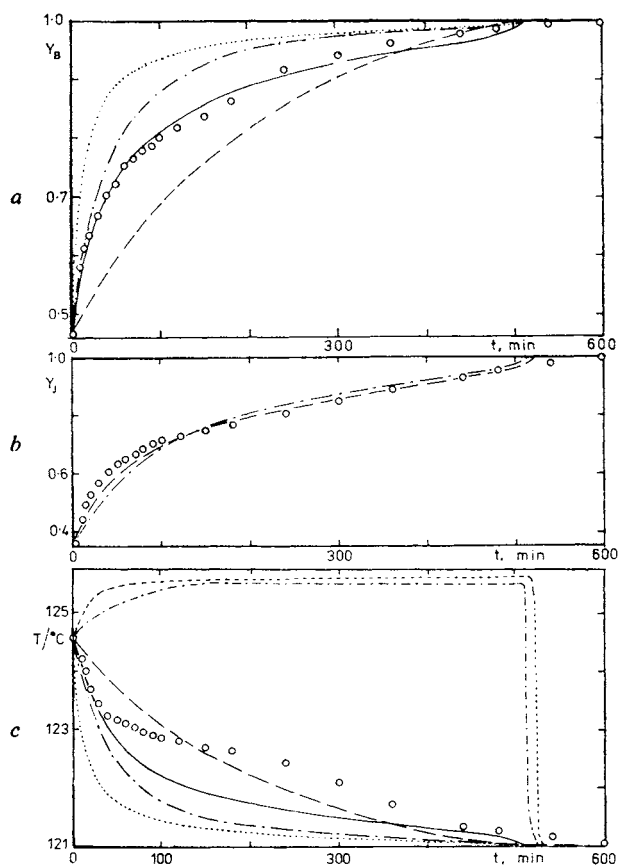


FIG. 2

Experimental run 2, designation as in **Fig. 1**

*Model* 5. For the given active core radius $\varphi^j$, $\tau$ and $Y_J^*$ have been computed as in models *3* and *4*. In the isothermal case the value $Y_B^*$ from Eqs (*34*) and (*44*) has been computed. In nonisothermal case the model equations have been solved numerically by the Newton method.

### RESULTS AND DISCUSSION

The values of the dimensionless parameters are in Table II. A part of the parameters in the model has been calculated *a priori*, while others had to be evaluated *a posteriori*. Parameters $\alpha_i$, $\alpha_k$, and $\varkappa_B$ have been estimated from the known reaction rate equation (*12*), parameters $\beta$, $Tg_B$, $Th_J$, $Bi$, and parameters $G$ and $\eta$ in the shell progressive models from the conditions at the start of the experiment (fresh catalyst) and parameter $Z_R$ from the experimental conditions. Parameters which have been eva-
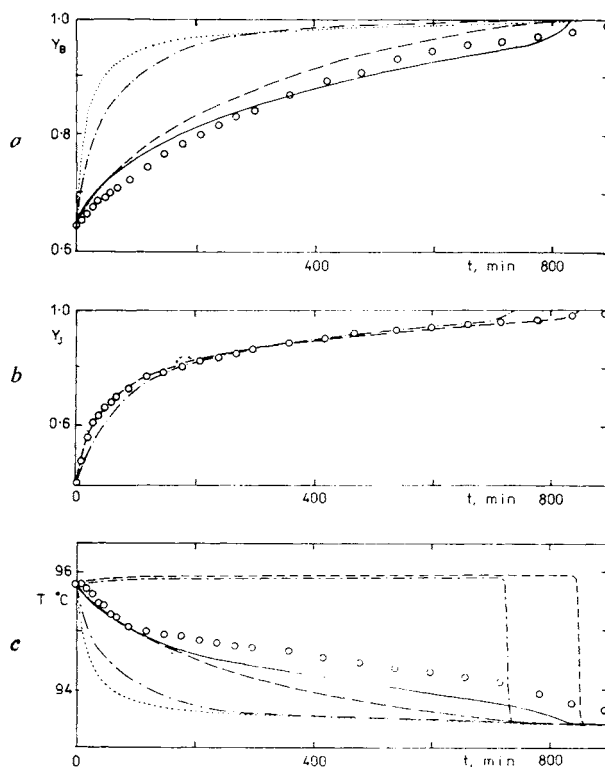


FIG. 3

Experimental run 3, designation as in Fig. 1

luated *a posteriori* are: parameter $G$ in diffusion models and $\omega$ in the shell progressive models.

Figs 1*a*, 2*a*, 3*a* illustrate the dependence of experimental benzene gas phase concentration in the reactor on time together with the computed ones for the above mentioned models and three experimental runs. The corresponding dependences for the thiophene are in Figs 1*b*, 2*b*, 3*b*. The dependences of temperature in the pellet center on time are in Figs 1*c*, 2*c*, and 3*c*. The differences between the diffusion and the shell progressive models are not significant, which follows from the high value of the Thiele modulus $Th_J$. The agreement of temperature is better under the assumption of constant temperature through the pellet.

The best result has been achieved by model *4* under the assumption of different Thiele modulus for benzene of active core and poisoned shell. In this paper they are used as adjustable parameters only. For all experimental runs the value of the Thiele modulus of the active core is much higher (almost by one order) than that for the shell (Table II). It leads to higher values of the diffusion coefficients in the shell. Apparently, in the shell only bulk diffusion in the pores takes place while in the core it is accompanied by adsorption on catalytic active sites. It is obvious that this affects diffusion rate. The temperature dependences of the Thiele modulus for benzene in core and shell and for thiophene are in Figs 4 and 5.

The aim of this work was to find the model of deactivation of one pellet applicable for computation of catalytic reactors. Since the diffusion and shell progressive deactivation models give practicaly the same results and diffusion models result in a very high computer time expenditure, shell progressive ones are more interesting from the practical point of view. By assuming that the effectiveness factor in the
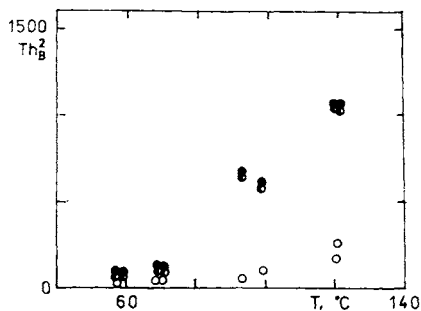


FIG. 4

Thiele modulus for benzene *vs* temperature. ◗ Models *1, 3*; ● Models *2, 4*; ○ Model *4* (shell)
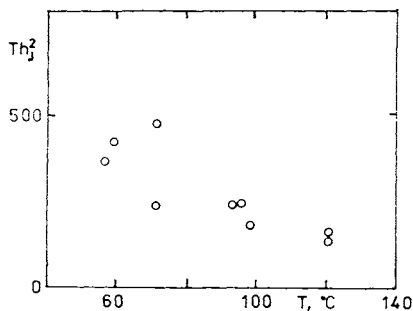
FIG. 5

Thiele modulus for thiophene *vs* temperature.

core is constant (model 5) the shell progressive model can be further simplified without decreasing its accuracy considerably.

## LIST OF SYMBOLS

| | |
|---|---|
| $a$ | adsorbed amount $(\text{mol m}^{-3})$ |
| $a^0$ | equilibrium adsorbed amount corresponding to the inlet conditions $(\text{mol m}^{-3})$ |
| $Bi$ | Biot criterium |
| $c$ | concentration $(\text{mol m}^{-3})$ |
| $C_p$ | heat capacity $(\text{J kg}^{-1} \text{ K}^{-1})$ |
| $D$ | diffusion coefficient $(\text{m}^2 \text{ s}^{-1})$ |
| $E$ | activation energy for catalytic reaction $(\text{J mol}^{-1})$ |
| $G$ | dimensionless parameter, see Eq. (39) |
| $(-\Delta H)$ | heat of reaction $(\text{J mol}^{-1})$ |
| $k_J$ | deactivation rate constant $(\text{m}^3 \text{ mol}^{-1} \text{ s}^{-1})$ |
| $k_S$ | rate constant of chemisorption $(\text{m s}^{-1})$ |
| $K_\infty$ | adsorption constant for benzene at $T \to \infty$ $(\text{m}^3 \text{ mol}^{-1})$ |
| $Q$ | adsorption heat of benzene $(\text{J mol}^{-1})$ |
| $r$ | radial position in a pellet $(\text{m})$ |
| $R$ | radius of a pellet $(\text{m})$ |
| $\boldsymbol{R}$ | gas constant $(\text{J mol}^{-1} \text{ K}^{-1})$ |
| $t$ | time $(\text{s})$ |
| $t^0$ | characteristic deactivation time $(\text{s})$ |
| $T$ | temperature $(\text{K})$ |
| $T_{\cdot}$ | bulk flow temperature $(\text{K})$ |
| $\Delta T_m$ | maximum temperature rise $(\text{K})$ |
| $Th$ | Thiele modulus |
| $V$ | volume of gas phase in the reactor $(\text{m}^3)$ |
| $\dot{V}$ | volumetric flow rate $(\text{m}^3 \text{ s}^{-1})$ |
| $W$ | mass of catalyst $(\text{kg})$ |
| $Y$ | dimensionless concentration |
| $Z_R$ | dimensionless parameter, see Eq. (39) |
| $\alpha$ | heat transfer coefficient $(\text{J m}^{-2} \text{ s}^{-1} \text{ K}^{-1})$ |
| $\alpha_i, \alpha_k, \beta, \varkappa_B$ | dimensionless parameters, see Eq. (45) |
| $\varepsilon$ | porosity of pellet |
| $\eta$ | effectiveness factor |
| $\vartheta$ | dimensionless temperature |
| $\lambda$ | thermal conductivity $(\text{J m}^{-1} \text{ s}^{-1} \text{ K}^{-1})$ |
| $\nu$ | stoichiometric coefficient |
| $\dot{\xi}_Z$ | reaction rate $(\text{mol m}^{-3} \text{ s}^{-1})$ |
| $\dot{\xi}_Z^0$ | reaction rate on the fresh catalyst corresponding to the inlet conditions $(\text{mol m}^{-3} \text{ s}^{-1})$ |
| $\dot{\Xi}$ | dimensionless reaction rate |
| $\varrho$ | pellet density $(\text{kg m}^{-3})$ |
| $\tau$ | dimensionless time |
| $\varphi$ | dimensionless radial position |
| $\phi$ | activity |

$\dot{\phi}$          deactivation rate

$\omega$          dimensionless parameter, see Eq. *(24)*

## Subcripts and exponents

B    benzene

H    hydrogen

j    active core

J    poison

*    surface

0    inlet stream

**REFERENCES**

1. Mikuš O., Pour V., Hlaváček V.: J. Catal. *48*, 98 (1977).
2. Lee J. W., Butt J. B., Downing D. M.: AIChE J. *24*, 212 (1978).
3. Butt J. B., Downing D. M., Lee J. W.: Ind. Eng. Chem., Fundam. *16*, 270 (1977).
4. Downing D. M., Lee J. W., Butt J. B.: AIChE J. *25*, 461 (1978).
5. Ho-Peng Koh, Hughes R.: AIChE J. *20*, 395 (1974).
6. Hegedus L. L., Petersen E. E.: Chem. Eng. Sci. *28*, 345 (1973); *28*, 69 (1973).
7. Khang S. J., Levenspiel O.: Ind. Eng. Chem., Fundam. *12*, 185 (1977).
8. Froment F. G., Bischoff K. B.: *Chemical Reactor Analysis and Design.* Wiley, New York 1979.
9. Lee H. H., Butt J. B.: AIChE J. *28*, 405 (1982).
10. Butt J. B.: Advan. Chem. Ser. *109*, 259 (1972).
11. Lee J. C. M., Luss D.: Ind. Eng. Chem., Fundam. *8*, 596 (1969).
12. Markoš J., Brunovská A., Ilavský J.: Unpublished results.